

Signal-to-noise ratio in direct-detection mid-infrared Random-Modulation Continuous-Wave lidar in the presence of colored additive noise

Adam Rybaltowski and Allen Taflove

Department of Electrical and Computer Engineering, Northwestern University, 2145 Sheridan Road, Evanston, IL 60208 USA

rybalt@ece.northwestern.edu, taflove@ece.northwestern.edu

Abstract: We have derived the signal-to-noise ratio in direct-detection Random-Modulation Continuous-Wave (RM-CW) lidar in the presence of colored additive noise. In contrast to a known formula derived for the photon shot-noise regime, which may adequately describe experimental conditions in the near-infrared, our result is applicable mainly at longer, mid-infrared wavelengths. Unlike the former formula, our result is explicitly dependent on the pseudorandom code (PRC) used for modulation. Three known modulation codes, the M-, A1-, and A2-sequence are compared and shown to have practically equivalent signal and noise properties (provided that clutter inherent in the A1- and A2-sequence is neglected), except that the M-sequence has a near-zero-frequency noise pickup that degrades its performance in real measurement systems. This difference provides an alternative explanation of a better performance of the A1-/A2-sequence in a previous experiment [3], carried out in the near-infrared. It suggests the presence of an additive noise component and thus some applicability of our result also in near-infrared lidar. A need for balanced sequences – particularly in the mid-infrared – is explained, although in a different way than previously suggested in near-infrared, photon shot noise-limited lidar. Additional, sinusoidal carrier modulation is considered and shown to have significant drawbacks. Our results allow comparison of given modulation sequences, and construction of improved ones. Interestingly, the improved sequences will possess less “random” characteristics, seemingly against the underlying concept of random modulation.

© 2001 Optical Society of America

OCIS codes: (010.3640) Lidar; (120.0280) Remote sensing; (280.0280) Remote sensing; (290.0290) Scattering; (300.0300) Spectroscopy

References and links

1. N. Takeuchi, N. Sugimoto, H. Baba, and K. Sakurai, “Random modulation cw lidar,” *Appl. Opt.* **22**, 1382-1386 (1983).
2. N. Takeuchi, H. Baba, K. Sakurai, and T. Ueno, “Diode-laser random-modulation cw lidar,” *Appl. Opt.* **25**, 63-67 (1986).
3. Ch. Nagasawa, M. Abo, H. Yamamoto, and O. Uchino, “Random modulation cw lidar using new random sequence,” *Appl. Opt.* **29**, 1466-1470 (1990).
4. J. L. Machol, “Comparison of the pseudorandom noise code and pulsed direct-detection lidars for atmospheric probing,” *Appl. Opt.* **36**, 6021-6023 (1997).
5. Y. Emery and C. Flesia, “Use of the A1- and the A2-sequences to modulate continuous-wave pseudorandom noise lidar,” *Appl. Opt.* **37**, 2238-2241 (1998).
6. C. M. Gittins, E. T. Wetjen, C. Gmachl, F. Capasso, A. L. Hutchinson, D. L. Sivco, J. N. Baillargeon, and A. Y. Cho, “Quantitative gas sensing by backscatter-absorption measurements of a pseudorandom code modulated $\lambda \sim 8\text{-}\mu\text{m}$ quantum cascade laser,” *Optics Lett.* **25**, 1162-1164 (2000).

7. A. B. Carlson, *Communication systems. An introduction to signals and noise in electrical engineering* (McGraw-Hill, 1986).
 8. S. Haykin, *Digital communications* (John Wiley & Sons, 1988).
-

1. Introduction

Lidar is a widely used optical technique of remote sensing. The sensed target can be - among others - a reflecting solid object or the atmosphere containing backscattering aerosols. Since range and angular resolution is normally required, a laser source capable of fast modulation or switching must be used. Typically, high peak-power ($\sim 1\text{-}10\text{MW}$) short-pulsed ($\sim 10\text{ns}$) lasers are used, but many applications call for compact laser sources (preferably solid-state/semiconductor), in which the maximum instantaneous power is significantly lower. This is particularly true in semiconductor and mid-infrared ($\sim 2\text{-}15\mu\text{m}$) lasers. Fortunately, these lasers can often operate at high duty-cycles and even continuously without severely compromising the maximum instantaneous power. This greatly compensates for its low level. The optimum overall lidar performance in such a case is achieved when the laser source is operated at as high a duty-cycle as possible. Then, to preserve range resolution, a special laser modulation and return signal demodulation sequence must be used. This technique is known as Random-Modulation Continuous-Wave (RM-CW) lidar [1-5]. It has been successfully applied to detect aerosols and particulate matter with the use of low-power cw near-infrared semiconductor lasers. However, a variety of applications - most notably spectroscopic measurements of physico-chemical parameters of the atmosphere - require mid-infrared wavelengths since atmospheric pressure-broadened ro-vibrational transitions in most molecules of interest are not properly resolved in the near-IR. Additionally, the near-IR transitions are much weaker, being overtones of the fundamental transitions in the mid-IR. Moreover, the atmosphere has broad windows of high transmission in the mid-IR. This has led to continued research efforts to develop mid-IR semiconductor lasers operating at high duty-cycles at or near room temperature, and to incorporate them into remote-sensing systems [6].

Therefore, a need arises to predict overall performance of the various types of mid-IR RM-CW lidar. At the core of such analysis is the signal-to-noise ratio of lidar return obtained with a given laser modulation sequence, atmospheric response function, and demodulation sequence, in the presence of a realistic noise that can be deduced from standard detector specifications. The purpose of this work is a derivation of this signal-to-noise ratio in the case of direct (i.e., optically non-coherent) detection lidar, and a comparison of the performance of known sequences (the M-, A1-, and A2-sequence). The M-sequence (also called the maximum shift-register sequence) is the most commonly used pseudo-random sequence [7,8]. It has been used for decades in spread-spectrum communications, an area closely related to RM-CW lidar through the use of correlation properties of pseudo-random sequences. In fact, the M-sequence can be defined by its correlation function (given in section 2.5.1) resulting from a feedback connection of a set of shift registers [8]. It was first applied to RM-CW lidar by Takeuchi *et al.* [1,2]. The A1-sequence can be viewed as a double-length M-sequence with inverted polarity in every other bit [3]; similarly, the A2-sequence is a quadruple-length M-sequence with inverted polarity in every other pair of adjacent bits [ibid.].

The derived signal-to-noise ratio is also instrumental in calculations of the sensing range and its limits in mid-IR direct-detection RM-CW lidar.

2. Signal-to-noise analysis in direct-detection mid-infrared RM-CW lidar

In the near-IR, the S/N ratio derived from Poissonian statistics of detected signal photons, background photons, and perhaps dark counts [1-4] often adequately describes practical detection regimes if the effect of demodulation is appropriately accounted for. This is particularly true when a photomultiplier tube (PMT) is used as a detector. Here, high internal gain, shunt resistance, and quantum efficiency combined with a low dark current allow

detection of photons close to the shot-noise limit, and thus derivation of the S/N ratio merely from the number of detected photons, assuming their Poissonian statistics. With an increasing wavelength, however, the above assumptions become invalid. Mid-IR detectors of sufficient and stable gain to overcome thermal noise do not exist. Further, background blackbody radiation can be stronger than the backscattered laser light. Finally, and most importantly, very low detector shunt resistance and/or high dark current typically yield much greater noise than thermal noise of the following amplifier/load. In this regime, the noise does not depend on the signal and is dominated by the detector. Then, our linear detection process allows treatment of the noise as being additive.

In practical systems, we also need to allow for the arbitrary spectral density (“color”) of the noise because its density strongly increases toward lower frequencies, typically below several kHz. Additionally, we will assume that the noise is stationary. This is a good assumption for practical purposes except near zero frequencies comparable to or lower than the inverse averaging time, where the stochastic mathematical model/treatment is not valid. Lastly, we will limit our analysis to direct-detection lidar, noting that a coherent superposition of the scattered wave with a local oscillator before square-law detection would violate our assumptions.

The entire model for our analysis is shown in Fig.1.

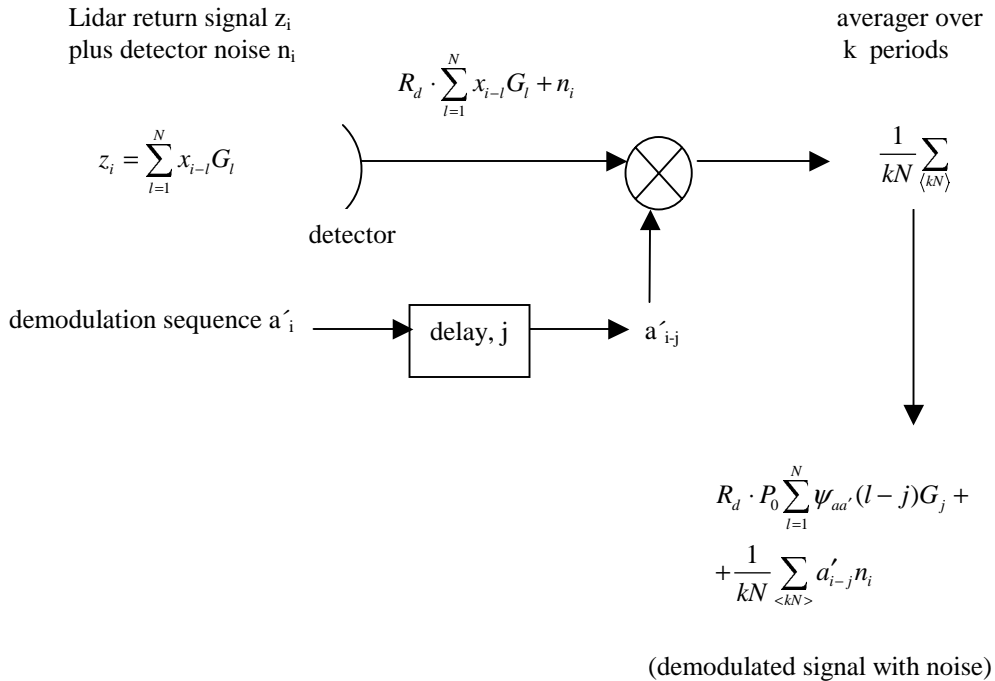


Fig. 1. Block diagram of signal-to-noise analysis of RM-CW lidar in presence of colored additive noise.

Following the references, x_i , z_i , and n_i are discrete-time counterparts of the respective continuous-time quantities, and G_i is the discrete-time counterpart of $g(t) \cdot \Delta t$, where

Δt is the sampling interval (chip length of the modulation waveform);

$x(t) = P_0 \cdot a(t)$ is the light power emitted into the atmosphere, where

P_0 is the laser output power when $a = 1$, and $a(t)$ is a (dimensionless) modulation waveform;

$a'(t)$, equal to +1 or -1 when a equals 1 or 0, respectively, is a demodulation waveform;

$g(t)$ is the atmospheric response function:

$$g(t) = \frac{c}{2} A_r \beta_r(R) T_r^2(R) Y(R) / R^2, \quad (1)$$

where

$$R = ct/2;$$

c is the velocity of light;

A_r – receiver's aperture area;

β_r – differential backscattering coefficient;

$T_r(R)$ – transmission coefficient to the distance R :

$$T_r(R) = \exp \left[- \int_0^R \alpha(r) dr \right] \quad (2)$$

(α - absorption coefficient),

$Y(R)$ – the crossover function, or the geometrical form factor, which is the fraction of the laser beam cross section covered by the receiver's field of view;

and n_i is the detector noise.

We have introduced the detector responsivity factor R_d . This factor converts the light power into the detector output signal, which – depending on the type of detector and amplifier used – can be voltage or current.

Finally, $\psi_{aa'}(j)$ is the (normalized) crosscorrelation function defined as

$$\psi_{aa'}(j) = \frac{1}{N} \sum_{i=1}^N a_i a'_{i+j}, \quad (3)$$

where N is the sequence length.

By varying the delay, j , the above scheme recovers G_j from any distance of interest. $G_j/\Delta t$ is then equal to the atmospheric response function g from the distance $R = (c \cdot j \cdot \Delta t)/2$. From G_j , $\beta_r(R)$ and its derivative parameters of the sensed medium can be determined. We are only concerned with the derivation of the S/N ratio in the measurement of G_j .

Since our detection and demodulation process is linear, and the noise is additive, we can calculate the output signal and noise separately.

2.1 The signal

The demodulated signal without noise is [3]

$$\frac{S_j^{(0)}}{N} = P_0 \sum_{l=1}^N \psi_{aa'}(l-j) G_j, \quad (4)$$

which for the M-sequence further equals

$$\frac{N+1}{2N} P_0 G_j \cong \frac{1}{2} P_0 G_j \quad (\text{large } N) \quad (5)$$

In an analogous manner, we have for the A1-sequence,

$$\frac{S_j^{(0)}}{2N} \cong P_0 \frac{N}{2N} G_j = \frac{1}{2} P_0 G_j, \quad (6)$$

and for the A2-sequence [ibid.],

$$\frac{S_j^{(0)}}{4N} \cong P_0 \frac{2N}{4N} G_j = \frac{1}{2} P_0 G_j \quad (7)$$

Note that the A1- and A2-sequence derived from the M-sequence of length N have a length of 2N and 4N, respectively.

Therefore, the M-, A1-, and A2-sequences possess equivalent signal properties in our S/N ratio analysis. Their different limitations and immunity to clutter do not affect our analysis.

The detector output signal for all of these sequences is equal to

$$\frac{R_d \cdot S_j^{(0)}}{N'} \cong \frac{1}{2} R_d \cdot P_0' G_j, \quad (8)$$

where we have substituted P_0' for P_0 to account for possible losses in light power between the telescope and the detector, and N' denotes the actual length of a given sequence.

2.2 The noise

To find the output noise, we will make a transition to continuous time and apply known tools of stochastic signal analysis [7]. The demodulated noise becomes

$$\frac{1}{kN} \sum_{\langle kN \rangle} a'_{i-j} n_i \rightarrow \frac{1}{T} \int_T a'(\tau) n(\tau) d\tau, \quad (9)$$

where $T = kN \cdot \Delta t$. This can be viewed as a moving average of a stochastic signal $a'(\tau)n(\tau)$ using a rectangular window of duration T.

Since we want to characterize $n(\tau)$ by its power spectral density, we will find the rms value of the output noise in the frequency domain. The power spectral density of the product $a'(\tau)n(\tau)$ is

$$G_{a'n}(f) = G_{a'}(f) * \frac{\eta(f)}{2}, \quad (10)$$

where

$$G_{a'}(f) = \mathfrak{S}\{R_{a'}(\tau)\} \quad (11)$$

is the power spectral density of the demodulation sequence $a'(t)$, $R_{a'}(\tau)$ is the normalized autocorrelation function of the demodulation sequence, and $\eta(f)$ is the positive-frequency noise power spectral density.

Since $R_{a'}(\tau)$ is periodic, its power spectral density can be represented as a Fourier series:

$$G_{a'}(f) = \sum_{n=-\infty}^{\infty} c_n \delta(f - nf_0), \quad (12)$$

where $f_0 = 1/T_0 = 1/(N \cdot \Delta t)$, and c_n are the Fourier coefficients of $R_a(\tau)$:

$$c_n = \frac{1}{T_0} \int_{T_0} R_{a'}(\tau) \exp(-j2\pi f_0 \tau) d\tau \quad (13)$$

Therefore,

$$G_{a'n}(f) = \int_{-\infty}^{\infty} \frac{\eta(\lambda)}{2} \sum_{n=-\infty}^{\infty} c_n \delta(f - nf_0 - \lambda) d\lambda = \sum_{n=-\infty}^{\infty} c_n \frac{\eta(f - nf_0)}{2} \quad (14)$$

The mean-square output noise is

$$\langle N_{out}^2(t) \rangle = \int_{-\infty}^{\infty} G_{a'n}(f) \cdot |H(f)|^2 df, \quad (15)$$

where $H(f)$ is the transfer function associated with the averager, which is a linear and time-invariant system. Here, we have assumed that the noise is stationary. $|H(f)|^2$ can be found from the impulse response function

$$h(t) = \frac{1}{T} \Pi\left(\frac{t}{T}\right), \quad (16)$$

which gives

$$|H(f)|^2 = |\mathcal{F}\{h(t)\}|^2 = \text{sinc}^2 fT \quad (17)$$

Therefore,

$$\langle N_{out}^2(t) \rangle = \sum_{n=-\infty}^{\infty} c_n \int_{-\infty}^{\infty} \frac{\eta(f - nf_0)}{2} \text{sinc}^2(fT) df \quad (18)$$

We can simplify this result if $T \cdot f_0 = (T/T_0) = k \gg 1$, that is, if the measurement/averaging is carried out over a large number of periods. The distribution $\text{sinc}^2 fT$ (of width $\sim 1/T$) can then be approximated by the $\delta(f)$ distribution:

$$\text{sinc}^2 fT = \frac{1}{T} T \text{sinc}^2 fT \rightarrow \frac{1}{T} \delta(f) \quad \text{for } k \rightarrow \infty, \quad (19)$$

which allows us to write the final formula for the output rms noise as

$$\sqrt{\langle N_{out}^2(t) \rangle} = \sqrt{\frac{1}{T} \sum_{n=-\infty}^{\infty} c_n \frac{\eta(nf_0)}{2}} \quad (20)$$

Here, we have used the fact that $\eta(f)$ is an even function.

2.3 The signal-to-noise ratio

Therefore, the signal-to-noise ratio in the measurement of the atmospheric response G_j is

$$\left(\frac{S}{N}\right)_j = \frac{\frac{1}{2}R_d \cdot P'_0 \cdot G_j}{\sqrt{\frac{1}{T} \sum_{n=-\infty}^{\infty} c_n \frac{\eta(nf_0)}{2}}} \quad (21)$$

To express R_d and η in terms of commonly used infrared detector specifications, we note that

$$D^*(f) = \frac{R_d \sqrt{A_d}}{\sqrt{\eta(f)/2}}, \quad (22)$$

where $D^*(f)$, the detectivity at frequency f , is a commonly used figure of merit for photodetectors, particularly in the mid-IR, and A_d is detector's area. Equation (21) then becomes

$$\left(\frac{S}{N}\right)_j = \frac{\frac{1}{2}P'_0 \cdot G_j}{\sqrt{\frac{1}{T} \sum_{n=-\infty}^{\infty} c_n \frac{\eta(nf_0)}{2R_d^2}}} = \frac{\frac{1}{2}P'_0 \cdot G_j}{\sqrt{A_d} \sqrt{\frac{1}{T} \sum_{n=-\infty}^{\infty} c_n \frac{1}{D^{*2}(nf_0)}}} \quad (23)$$

As we can see, strict prediction of the signal-to-noise ratio requires knowledge of $\eta(f)$ or $D^*(f)$ in a range of frequencies from DC to $\sim 1/\Delta t$, whereas D^* at only one frequency is available in routine detector specifications.

For noise whose power spectral density $\eta(f)$ does not change throughout the range of frequencies where c_n is significant (that is, from DC to $\sim 1/\Delta t$), we can simplify the above expression noting that

$$\sum_{n=-\infty}^{\infty} c_n = R_d \cdot (\tau = 0) = 1 \quad (24)$$

Therefore, in the case of white noise, Eq. (21) reduces to

$$\left(\frac{S}{N}\right)_j = \frac{\frac{1}{2}R_d \cdot P'_0 \cdot G_j}{\sqrt{\frac{\eta}{2T}}} = \frac{\frac{1}{2}P'_0 \cdot D^* \cdot G_j}{\sqrt{A_d} \sqrt{\frac{1}{T}}} \quad (25)$$

2.4 Comparison to the photon shot-noise regime

We can now compare the result of Eq. (25) to that derived by Takeuchi *et al.* [1,2] for the M-sequence in the case of signal and background photon shot-noise-limited measurements, which is a realistic approximation in near-IR lidar:

$$\left(\frac{S}{N}\right)_{RM} = \frac{\sqrt{k}\sqrt{\xi} \cdot IP_0\tilde{G}_j}{\sqrt{N}\sqrt{IP_0\bar{G} + \bar{b}}}, \quad (26)$$

where

$l \approx N/2$ for the M-, A1-, and A2-sequences;

N is the sequence length;

k is the number of periods of averaging;

\bar{b} is the background radiation power;

$\xi = \Delta t \cdot \eta_Q / h\nu$ is the conversion constant from light power to photoelectron number, where

η_Q is the detector's quantum efficiency,

h is Planck's constant,

ν is the light frequency;

Here, the excess noise factor (typically ~ 2 to 3 in PMTs), has been neglected.

For a meaningful comparison, we will reduce Eq. (26) to the case $IP_0\bar{G} \gg \bar{b}$, that is, background photon shot-noise-limited detection:

$$\left(\frac{S}{N}\right)_{RM} \rightarrow \frac{\frac{1}{2}\xi P_0\tilde{G}_j}{\sqrt{\frac{\bar{b}\xi}{kN}}} \quad (27)$$

Essentially, our result – Eq. (25) – is the same as Eq. (27) except that the denominators describe noise of a different nature. Specifically,

$\sqrt{\frac{\bar{b}\xi}{kN}}$ is the Poissonian noise of background photons detected during the measurement interval of k cycles, normalized consistently with the signal (i.e., divided by kN), and

$\sqrt{\frac{\eta}{2T}}$ is the rms detector noise of positive-frequency power spectral density η in the noise-equivalent bandwidth of $1/2T$, corresponding to time-averaging over a period of T .

2.5 Performance comparison of the M-, A1-, and A2-sequence in the presence of colored noise

Returning to the general case of colored noise, we will evaluate the S/N ratio given by Eq. (21) for three specific sequences: M, A1, and A2. We have found that signal properties (the numerator in Eq. (21)) are described by the crosscorrelation function between the modulation and the demodulation sequence, and are practically identical for all of these sequences. Noise properties (the denominator in Eq. (21)) are described by the autocorrelation function of the demodulation sequence.

2.5.1 The M-sequence

The autocorrelation function $R_a^{(M)}(\tau)$ and its Fourier coefficients for the M-sequence are known to be [8]

$$R_a^{(M)}(\tau) = \left(1 + \frac{1}{N}\right) \sum_{k=-\infty}^{\infty} \Lambda\left(\frac{\tau - kNT_c}{T_c}\right) - \frac{1}{N} \quad (28)$$

and

$$c_0^{(M)} = \frac{1}{N^2}; \quad c_n^{(M)} = \frac{N+1}{N^2} \text{sinc}^2 \frac{n}{N} \cong \frac{1}{N} \text{sinc}^2 \frac{n}{N}, \quad n \neq 0 \quad (29)$$

where T_c , called the chip length, equals Δt , and the fundamental frequency ($n=1$) is $f_0=1/(NT_c)$.

2.5.2 The A1- and A2-sequence

The autocorrelation function $R_a^{(A1)}(\tau)$ of the A1-sequence [3] of length $2N$ (obtained from the M-sequence of length N) can be written as

$$R_a^{(A1)}(\tau) = \frac{1}{N} + \sum_{k=-\infty}^{\infty} \left\{ \left(1 + \frac{1}{N}\right) \left[\Lambda\left(\frac{\tau - k2NT_c}{T_c}\right) - \Lambda\left(\frac{\tau - (2k+1)NT_c}{T_c}\right) \right] - \frac{2}{N} \Lambda\left(\frac{\tau - k2T_c}{T_c}\right) \right\} \quad (30)$$

As in our signal analysis, for large N , we can neglect the low-amplitude and high-frequency "ripple" described by the last term in the above equation. The Fourier coefficients then become

$$c_n^{(A1)} = \frac{N+1}{N} \text{sinc}^2 \left[\left(n - \frac{1}{2}\right) \frac{1}{N} \right] \cong \frac{1}{N} \text{sinc}^2 \left[\left(n - \frac{1}{2}\right) \frac{1}{N} \right] \quad (31)$$

and the fundamental frequency is now $f_0 = 1/(2NT_c)$.

For large N , the results for the A2-sequence of the same length as the A1-sequence are identical.

2.5.3 Sequence parameters and performance comparison

To perform a sensible comparison of the S/N properties of the three sequences under consideration, we need to specify their parameters: the chip length and the total length. We consider the following choice of parameters to be optimal.

The M-sequence of length N should be compared to the A1-sequence of length $2N$ and the A2-sequence of length $2N$. This choice implies that the A2-sequence is derived from the M-sequence of half the length, $\cong N/2$. Further, the chip lengths of all of these three sequences should be the same. This choice is dictated by, and satisfies, the following criteria:

- The range resolution obtained with any of these sequences of chosen parameters is the same. This also allows maintaining the same signal properties (the same atmospheric response G_j).
- The bandwidth required to realize specified modulation patterns is the same for each sequence.

- The unambiguous range as measured by the spacing between two adjacent peaks associated with signal properties is the same for each sequence.

As a consequence, however, we have to accept two minor differences between such chosen sequences:

- The fundamental frequency f_0 of the A1/A2 sequence is half that of the M-sequence.
- The “ripple” in the autocorrelation and crosscorrelation function of the A2-sequence, as measured by the ratio of the amplitudes of the small (“ripple”) peaks to the large (signal-related) peaks, is twice that of the A1-sequence ($2/N$ compared to $1/N$).

This nonzero correlation observed between major peaks of the crosscorrelation function is responsible for undesirable pickup of signals from different ranges (clutter), and degrades the signal properties of the A1- and A2-sequences in unfavorable conditions [5]. Since we have excluded this effect in our signal analysis, and have shown its negligible contribution to overall noise, the given choice of sequence parameters (chip length and total length) combined with our results show that the A1- and A2-sequences are equivalent in terms of their signal and noise properties.

Therefore, we only need to compare the noise properties of the M-sequence of length N to those of the A1-sequence of length $2N$ using Eq. (29) and Eq. (31). First, we note that

$$\sum_{n=-\infty}^{\infty} c_n \frac{\eta(nf_0)}{2}$$

is a weighted average of all $\eta(nf_0)$. Furthermore, this average is properly normalized, since – for all demodulation sequences – their normalized autocorrelation is equal to one at $\tau=0$ (Eq. (24)). Therefore, the noise performance of the various demodulation sequences can be qualitatively compared by plotting the Fourier coefficients c_n for each sequence (see Fig.2).

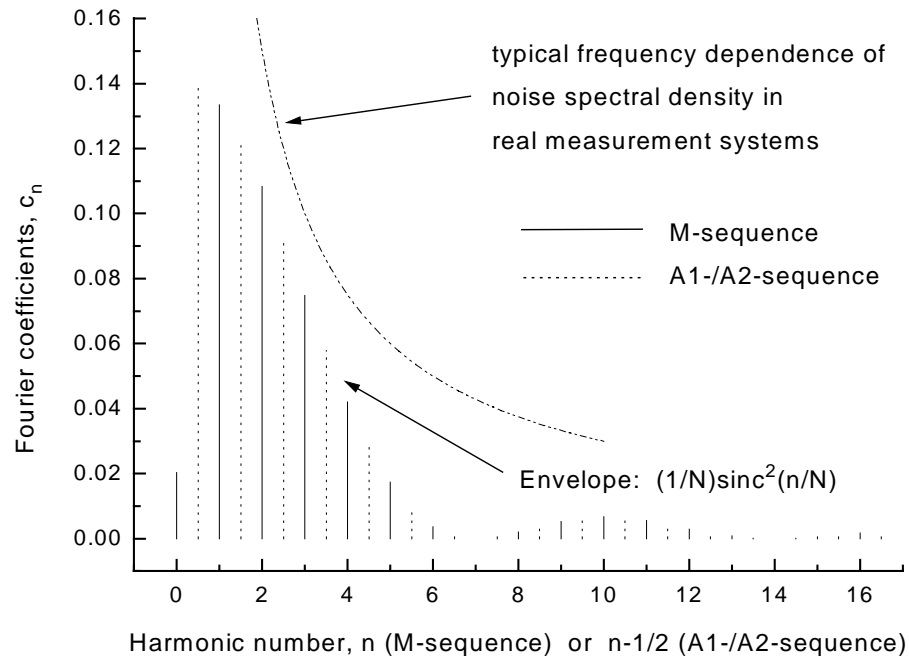


Fig. 2. Comparison of noise pickup distribution of M-sequence and A1-/A2-sequence; $N=7$.

As we can see from Fig.2, the noise properties of the M-, A1-, and A2-sequences in our approximation of $k \rightarrow \infty$ are practically the same, except that the M-sequence has a nonzero DC noise pickup. In practical electronic systems, where the noise spectral density strongly increases toward low frequencies (typically like $\sim 1/f$ below a few kHz), this difference can result in superior performance of the A1/A2-sequence, and could explain a better S/N ratio in an experimental comparison carried out by Nagasawa *et al.*[3].

Since the limiting case $k \rightarrow \infty$ (infinite number of periods) is not strictly satisfied in practice, it is worthwhile to notice that the effect of finite k can be incorporated as windowing. Indeed, in Eq. (18), we have $\text{sinc}^2 fT$ (T is the averaging time) rather than $(1/T)\delta(f)$. As a result, the line spectra described by the Fourier coefficients c_n are in general windowed, frequency-broadened to $\sim 1/T$. Therefore, in practical systems, our concern is the pickup of near-zero-frequency noise (down to $\sim 1/T$) rather than “DC” noise. [In fact, our framework of stochastic noise analysis is not valid for frequencies lower or comparable to $1/T$, although the description of DC noise pickup is qualitatively correct.] A semi-quantitative analysis shows that the S/N ratio is an order of magnitude greater in the A1- or A2-sequences compared to the M-sequence in typical experimental conditions (sequence length $N=1000$; chip length $T_c=30\text{ns}$; integration time $T=3\text{s}$; and $1/f$ noise spectral density). The ~ 5 -times greater S/N ratio in the A2-sequence compared to the M-sequence that was observed in an experiment carried out by Nagasawa *et al.* [3] using a near-IR laser is in satisfactory agreement with our estimation. This agreement is reasonable taking into account that the performance differences between pseudo-random sequences are associated with the additive colored noise component, which is generally less pronounced at shorter (near-IR)

wavelengths. The advantage of the A1- or A2-sequence over the M-sequence by a factor of 9 in the S/N ratio corresponds to a 3-fold improvement in the maximum lidar sensing range.

2.5.4 Effect of imbalance on overall performance

As we have established that a DC component in the spectrum of the autocorrelation function of a demodulation sequence is highly undesirable, it would be worthwhile to relate it to some simple property of the sequence. Below, we show that this DC component c_0 is uniquely related to the imbalance property of the demodulation sequence:

$$\begin{aligned} c_0 &= \frac{1}{T_0} \int_{T_0} R_{a'}(\tau) d\tau = \frac{T_c}{T_0} \sum_{i=0}^{N-1} \psi_{a'}(i) = \frac{1}{N} \sum_{i=0}^{N-1} \psi_{a'}(i) = \\ &= \frac{1}{N} \sum_{i=0}^{N-1} \sum_{j=1}^N \frac{1}{N} a'_j a'_{j+i} = \left(\frac{\sum_{i=1}^N a'_i}{N} \right)^2 \end{aligned} \quad (32)$$

For the M-sequence, $\sum_{i=1}^N a'_i = 1$, which gives $c_0 = (1/N)^2$, in agreement with $c_0^{(M)}$ given by Eq.

(29). By definition, an imbalanced sequence has $\sum_{i=1}^N a'_i \neq 0$, and therefore yields a nonzero (or near-zero-frequency) noise pickup, whereas a balanced sequence yields none.

Interestingly, the requirement of balance in a sequence that maximizes the signal-to-noise ratio in the presence of a typical colored noise (i.e., increasing toward low frequencies) is in an apparent contradiction with the requirement of “randomness.” This is because an ideal random sequence would have a frequency-independent spectral density at the low-frequency end. Therefore, sequences that are optimal for practical RM-CW lidar applications will not possess ideal “random” or even “pseudorandom” properties.

2.6 Random modulation on a sinusoidal carrier

Our previous discussion dealt with baseband transmission, that is, the light power was modulated only by the pseudorandom sequence. The modulation spectrum and the noise pickup extended from \sim DC to \sim 1/T_c, covering the region of highest noise density in practical systems. To avoid this spectral coincidence, we could employ additional modulation with a sinusoidal carrier, which would shift the modulation spectrum and noise pickup to higher frequencies where the noise density is usually much lower. This would, however, degrade the signal properties of the entire system, as we show below.

Let the carrier- and PRC-modulated output be

$$a(t) \rightarrow a(t) \left[\frac{1}{2} + \frac{1}{2} \cos(2\pi f_m t + \phi_m) \right], \quad (33)$$

where $f_m \gg 1/T_c$ is the carrier frequency, such that the maximum instantaneous laser output power remains the same. The demodulation waveform is

$$a'(t) \rightarrow a'(t) \cos(2\pi f_m t + \phi'_m) \quad (34)$$

Since $a'(t)$ is symmetric about the zero level, the constant component $1/2$ in $a(t)$ can be neglected as it vanishes upon demodulation.

The noise pickup distribution is given by the Fourier spectrum of the autocorrelation function

$$R_{a',m}(\tau) = R_{a'}(\tau)R_m(\tau) = R_{a'}(\tau)\frac{1}{2}\cos 2\pi f_m \tau \quad (35)$$

$$\begin{aligned} \mathfrak{S}\{R_{a',m}(\tau)\} &= \mathfrak{S}\{R_{a'}(\tau)\} * \mathfrak{S}\left\{\frac{1}{2}\cos 2\pi f_m \tau\right\} = \\ &= \mathfrak{S}\{R_{a'}(\tau)\} * \frac{1}{2} \frac{\delta(f-f_m) + \delta(f+f_m)}{2} = \\ &= \frac{1}{4}G_{a'}(f-f_m) + \frac{1}{4}G_{a'}(f+f_m) \end{aligned} \quad (36)$$

As expected, carrier modulation shifts the center of the noise pickup distribution from 0 to $\pm f_m$.

Similarly, the crosscorrelation becomes

$$\begin{aligned} R_{a',am}(\tau) &= \left\langle a'(t)a(t+\tau)\cos(2\pi f_m t + \varphi'_m)\frac{1}{2}\cos[2\pi f_m(t+\tau) + \varphi_m] \right\rangle = \\ &= \frac{1}{4}R_{a'a}(\tau)\cos(2\pi f_m \tau + \varphi_m - \varphi'_m) \end{aligned} \quad (37)$$

Therefore, in the presence of carrier modulation (in addition to pseudorandom code modulation), Eq. (21) is still valid if the numerator (the demodulated signal) is multiplied by $(1/4)\cos(2\pi f_m \tau + \varphi_m - \varphi'_m)$ and we substitute

$$c_n \rightarrow \frac{1}{4}c_{n-n'} + \frac{1}{4}c_{n+n'} \quad (38)$$

with $n' = f_m/f_0$ in the denominator (demodulated noise).

Thus, the envelope of the demodulated signal-to-noise ratio in the case of carrier modulation is $4/\sqrt{2} = 2\sqrt{2} \cong 2.83$ times lower than in the case of baseband (no carrier) modulation, using only a pseudorandom sequence. A factor of 2 is due to the twice lower average emitted laser power, and a factor of $\sqrt{2}$ is due to the twice shorter effective noise averaging time.

Another significant drawback of carrier modulation is the requirement of much higher modulation and detection bandwidth ($f_m \gg 1/T_c$) and related signal processing power, and perhaps also PRC – carrier synchronization. Furthermore, despite these increased requirements, the range resolution is not enhanced. The range resolution is still determined only by the crosscorrelation length of the random component of modulation, which is a pseudorandom modulation code.

3. Summary and conclusions

Our results allow calculation of the signal-to-noise ratio in direct detection Random-Modulation Continuous-Wave lidar in the additive noise regime. Our theory accounts for an arbitrary noise spectral density and the basic properties of the system: maximum instantaneous laser power, detector's detectivity and area, atmospheric response function, autocorrelation function of the demodulation sequence, and its crosscorrelation function with the modulation sequence.

The derived S/N ratio is instrumental in calculations of the sensing range and its limits in mid-IR direct-detection RM-CW lidar. This, however, requires specifying the atmospheric response function for a given type of lidar, and is a subject of future work.

Since addition of a sinusoidal carrier is shown to have significant drawbacks over baseband modulation, the results are most useful in a comparison of existing pseudorandom sequences and in devising new ones. Three known sequences, the M-, A1-, and A2-sequences, are shown to have practically equivalent signal and noise properties. Differences arise only due to clutter inherent in the A1- and A2-sequences, and the fact that the M-sequence is imbalanced and thus has a near-zero-frequency noise pickup. The imbalance degrades the performance of the M-sequence in practical systems with an additive noise component in which the noise density strongly increases toward lower frequencies. This result provides an alternative explanation of better performance of the A2-sequence in an experimental comparison to the M-sequence if we allow for the existence of an additive noise component [3]. We believe that the imbalance property plays no role in photon shot-noise-limited detection. Demodulation can be viewed as a functional on a random, Poissonian incidence of photons, with the mean related to imbalance, but not to the variance. It is best illustrated by any balanced sequence, in which the mean noise is zero, while its variance is not. The S/N ratio has not been previously derived for such sequences.

Since generally the contribution of the additive component to noise strongly increases with wavelength, so does the importance of balance in the demodulation sequence. While at near-IR wavelengths an experiment has shown a few times greater S/N ratio in a balanced sequence compared to the M-sequence [ibid.], this advantage would most likely be much greater at mid-IR wavelengths. It puts a constraint of balance on the design of new sequences for RM-CW lidar, particularly in the mid-IR. Interestingly, such sequences will possess less "randomness" than the modulation sequences originally proposed for random modulation.